

# Fourier Transform Analysis on Random Quasi-Phase-Matched Nonlinear Optical Interactions

Kai Zhong , Sijia Wang, Kefei Liu , Degang Xu , and Jianquan Yao 

**Abstract**—The Fourier transform method is adopted to analyze random quasi-phase matched (RQPM) nonlinear frequency conversion problems in polycrystalline materials. By treating the material as random signals of effective nonlinear coefficient ( $d_{\text{eff}}$ ) along the beam path, fast Fourier transform (FFT) operations directly produce the generated field amplitude versus spatial frequency mismatch ( $\Delta k/2\pi$ ), which relates to all the possible RQPM nonlinear interactions. Thus, the RQPM bandwidth is intuitive from the wavelength-dependent results. More importantly, the Fourier transform treatment greatly decreases the computational amount by orders compared with the traditional step-by-step integration method. The quantitative simulation of RQPM difference frequency generation (DFG) with three variable wavelengths is realized for the first time.

**Index Terms**—Fourier transform treatment, nonlinear frequency conversion, polycrystalline material, random quasi-phase matching.

## I. INTRODUCTION

NONLINEAR optical frequency conversion that mainly relies on the  $\chi^{(2)}$  susceptibility of non-centrosymmetric crystals provides diverse methods for laser wavelength extension, where phase matching (PM) is a critical factor for efficient conversion. Birefringent PM is fulfilled by special polarizations, crystal orientation or working temperature to manipulate the refractive indices (velocities) of three interaction waves. The other technique requires the crystal to periodically invert the sign of effective nonlinear coefficient ( $d_{\text{eff}}$ ) every coherence length, known as quasi-phase matching (QPM). Both birefringent PM and QPM have been extensively studied in theory, experiment, and device, and are now widely used to generate new laser lines from ultraviolet to far infrared.

A relatively new PM approach that is defined as random quasi-phase matching (RQPM) was proposed more than a decade ago [1]. It is realized in disordered polycrystals especially

the isotropic nonlinear medium (ZnSe, ZnS, etc.) with wide transparency and high  $\chi^{(2)}$  susceptibility. RQPM is costless and independent to material orientation and input laser polarization, thus it possesses an extremely large bandwidth. During the past few years, RQPM nonlinear interactions driven by femtosecond lasers have received increasing attention to get broadband coherent mid-infrared (MIR) laser sources [2]–[6]. The RQPM efficiency can be comparable to traditional PM and QPM methods [3]–[5].

While remarkable experimental achievements are arising in laboratories, modeling and simulating the RQPM process have been challenging for a long time because of the randomness. Usually, a bulk polycrystalline material is created from sintering and pressing tiny grains with random morphology, resulting in random paths and so are the interactions across an input laser beam spot. Early theories assumed the grain size to follow Gaussian distribution with averaged  $d_{\text{eff}}$ , from which some basic rules for RQPM like the optimal grain size and the conversion efficiency versus interaction length, were concluded [1], [7]. Comprehensive models were also proposed for harmonic and supercontinuum generation pumped by ultrashort pulses [8], [9]. Recently, professional ceramic modeling tools were introduced to create realistic samples, and the reliable statistical analyzation by full-space scanned integrations allowed us to see RQPM more clearly through the second harmonic generation (SHG) process [10]. Unfortunately, the computational amount was tremendous and the explanation of the ultrabroad bandwidth was not intuitive enough. In addition, the calculation complexity prevents personal computers from performing wavelength-dependent simulations on more complicated processes, e.g., difference frequency generation (DFG) which involves three variable wavelengths.

In this paper, a Fourier transform treatment method is proposed for RQPM simulation and its effectiveness is demonstrated. By regarding the random  $d_{\text{eff}}$  along the beam path as a signal, Fourier transform converts it into the space of spatial frequency mismatch ( $\Delta k/2\pi$ ) relating to various wavelength-dependent nonlinear processes. The explanation for the ultrabroad bandwidth of RQPM can also be given from the point of  $\Delta k/2\pi$  connecting to the interaction wavelengths. Benefiting from the efficient discrete Fourier transform (DFT) algorithm, the RQPM DFG process covering the transparent range of polycrystalline ZnSe was studied for the first time, which greatly helps to determine the optimal scheme for a widely tunable MIR source. Compared with the step-by-step integration method,

Manuscript received November 3, 2021; revised November 27, 2021; accepted December 8, 2021. Date of publication December 13, 2021; date of current version December 22, 2021. This work was supported in part by the National Natural Science Foundation of China under Grant 62175184, in part by the Natural Science Foundation of Tianjin City under Grant 18JCYBJC16700, and in part by the Open Fund of Key Laboratory of Optoelectronic Information Technology, Ministry of Education under Grant 2021KFKT010. (Corresponding author: Kai Zhong.)

The authors are with the Institute of Laser and Optoelectronics, School of Precision Instruments and Optoelectronics Engineering, Tianjin University, Tianjin 300072, China, and also with the Key Laboratory of Optoelectronics Information Technology, Ministry of Education, Tianjin 300072, China (e-mail: zhongkai@tju.edu.cn; wangsjia@tju.edu.cn; liukefei@tju.edu.cn; xudegang@tju.edu.cn; yaojianquan@tju.edu.cn).

Digital Object Identifier 10.1109/JPHOT.2021.3134666

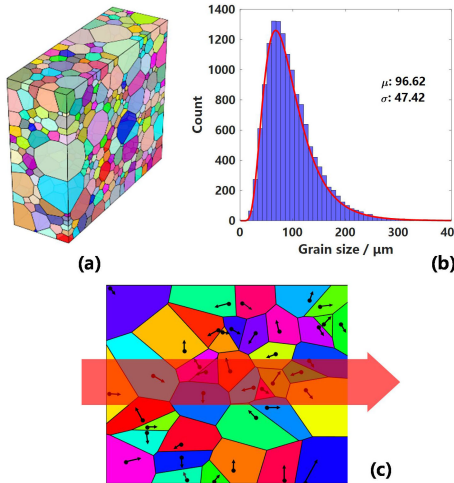


Fig. 1. A polycrystalline ZnSe sample and a passing laser beam. (a) Morphology of the sample. (b) Statistical histogram of the grain-size distribution. (c) A cross section of laser beam in the material. The black arrows show the optical axes of the grains.

the Fourier transform method could reduce the computation by orders and should be an effective tool for RQPM modeling.

## II. FOURIER TRANSFORM TREATMENT OF RQPM: CONCEPT

A realistic polycrystalline ZnSe model was generated by the professional software Neper and the statistical grain size follows the lognormal distribution [10], [11], as shown in Fig. 1(a) and 1(b). The preset average grain size ( $\mu = 95 \mu\text{m}$ ) and standard deviation ( $\sigma = 48 \mu\text{m}$ ) were in good agreement with that of the actual generated model ( $\mu = 96.62 \mu\text{m}$ ,  $\sigma = 47.42 \mu\text{m}$ ). Considering an SHG process with a certain fundamental beam size described in Fig. 1(c), the waves propagate through a series of grains and the beam path over the cross section varies with position.

Microscopically, RQPM SHG is affected by two random factors: one is the random morphological distribution (size and shape) and the other is the random orientation of the grains along the path. The former determines the interaction length and the latter corresponds to  $d_{\text{eff}}$  of every grain. Then the small-signal plane-wave solution of the second-harmonic electric field is

$$E_{2\omega} = \frac{i\omega E_{\omega}^2}{cn_{2\omega}} \sum_{n=1}^m \int_{z_{n-1}}^{z_n} d_{\text{eff},n} e^{-i\Delta k z} dz \quad (1)$$

where the beam is assumed to be along the laboratory  $z$  axis,  $E_{\omega}$  is the fundamental electric field,  $\Delta k$  denotes the phase mismatch,  $c$  is the light speed in vacuum,  $n_{2\omega}$  is the refractive index of the second harmonic wave,  $m$  is the total grain number along the beam path,  $z_0 = 0$  represents the incident plane of the material, and  $z_n$  and  $d_{\text{eff},n}$  are the exit coordinate and effective nonlinear coefficient of the  $n^{\text{th}}$  grain ( $n$  is integer and  $1 \leq n \leq m$ ), respectively. The integration range from  $z_{n-1}$  to  $z_n$  is the beam path in the  $n^{\text{th}}$  grain.

From the integration of (1), it is clear that  $d_{\text{eff},n}$  and  $z_n - z_{n-1}$  are the main concerns to acquire  $E_{2\omega}$ . The detailed spatial morphology of every path can be extracted after meshing the

model to provide  $z_n - z_{n-1}$ , while  $d_{\text{eff},n}$  is given by the random coordinate transformation [8], [10]. Then the simulation is straightforward to yield conversion efficiency, wavelength dependence, etc., by performing full-scale-scanning step-by-step integrations of the polycrystalline sample. However, such a direct method is accompanied by a large volume of calculation. Taking a  $1 \text{ mm} \times 1 \text{ mm} \times 0.5 \text{ mm}$  sample with the meshing step of  $10 \mu\text{m}$  for example,  $100 \times 100 \times 50$  integrations are required to obtain the full distribution of the SHG field. To study the SHG bandwidth, the computational amount is increased proportionally to the wavelength points involved. The investigation of a DFG process where three wavelengths are all variable is almost impractical with this method.

A new concept to study the RQPM process is to convert the spatial distribution of  $d_{\text{eff},n}$  into the  $\Delta k$  space by DFT which is used in dealing with signals that are either periodic or aperiodic [12]–[15]. From the view that the grains in a polycrystal provide massive reciprocal lattice vectors to compensate for the phase mismatch  $\Delta k$ , Fourier transform looks at all kinds of three-wave interactions at once and greatly simplifies the RQPM analyzation. Fourier transform of  $d_{\text{eff}}$  along the beam path is carried out by

$$\mathcal{F}(\Delta k) = \int d_{\text{eff}}(z) e^{-i\Delta k z} dz \quad (2)$$

It is noticeable that (2) is contained in (1) for the SHG problem. When a different nonlinear interaction (e.g., DFG) is considered, only the left part outside the bracket in (1) is different. If we define

$$\kappa_{\text{SHG}} = \frac{i\omega E_{\omega}^2}{cn_{2\omega}} \quad (3)$$

as a coefficient for SHG, such a coefficient for DFG is similarly written as

$$\kappa_{\text{DFG}} = \frac{i\omega_3 E_1 E_2^*}{cn_3} \quad (4)$$

where  $\omega_3 = \omega_1 - \omega_2$  is the generated frequency.

Then the electric fields for SHG and DFG are uniformly expressed as

$$E_{\text{SHG/DFG}} = \kappa_{\text{SHG/DFG}} \mathcal{F}(\Delta k) \quad (5)$$

Fourier transform is a standard part of most mathematical packages in the form of fast Fourier transform (FFT) for efficient calculation. However, it is important to notice that there is a difference of  $2\pi$  between the FFT operation and (2), thus  $\Delta k$  should be converted into  $\Delta k/2\pi$ , which is named as spatial frequency mismatch here for clarity.

As the first example, the RQPM nonlinear interaction in a polycrystalline ZnSe sample with the thickness of  $0.5 \text{ mm}$  is studied. Fig. 2 demonstrates the case of a single-path interaction when the incident beams are  $x$ -polarized. Whether the polarization of the generated wave is  $x$  or  $y$ , there are 51 discrete data points of  $d_{\text{eff}}$  along the beam path ( $z$  axis) when the meshing step (sampling period) is  $10 \mu\text{m}$  (sampling frequency  $0.1 \mu\text{m}^{-1}$ ), as shown in Fig. 2(a). According to the Nyquist sampling rule [15], the highest  $\Delta k/2\pi$  is  $0.05 \mu\text{m}^{-1}$  ( $0.1 \mu\text{m}^{-1} / 2$ ). Fig. 2(b) gives the squared FFT amplitude of the “random signal” in Fig. 2(a),

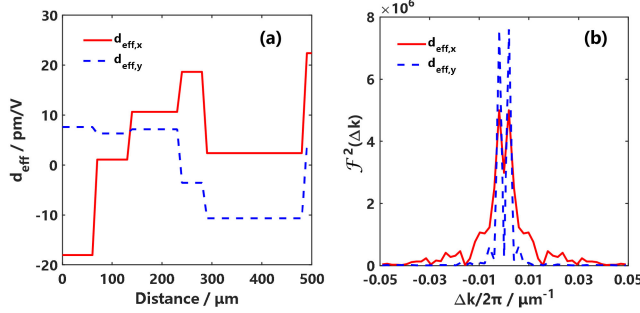


Fig. 2. FFT treatment of RQPM interactions along a single beam path. (a) Distribution of  $d_{\text{eff}}$ . (b)  $\mathcal{F}^2(\Delta k)$ , the squared FFT amplitude to (a).  $d_{\text{eff},x}$  and  $d_{\text{eff},y}$  are the effective nonlinear coefficients related to generated signal waves polarizing along the  $x$  and  $y$  axes, respectively.

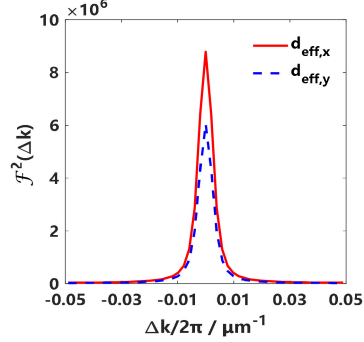


Fig. 4. Monte Carlo analysis of polycrystalline samples with a quarter million paths: the averaged  $\mathcal{F}^2(\Delta k)$ .

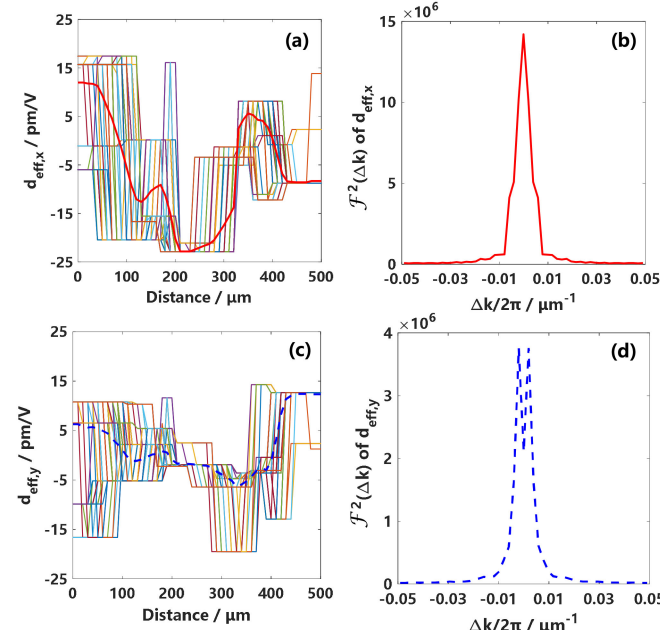


Fig. 3. FFT treatment of RQPM interaction over a beam cross section with 100 beam paths. (a) and (c) are the distributions of  $d_{\text{eff}}$  for  $x$ - and  $y$ -polarized signals. (b) and (d) are the averaged  $\mathcal{F}^2(\Delta k)$  to (a) and (c), respectively.

which can reflect the conversion efficiency. The leaps on the curves indicate that certain nonlinear processes are relatively efficient due to the phase compensation provided by specific grains along the beam path.

If we consider a practical laser beam size of  $100 \mu\text{m} \times 100 \mu\text{m}$ , there are 100 parallel beam paths since the meshing step is  $10 \mu\text{m}$ . The distributions of  $d_{\text{eff}}$  for each beam path are shown as thin lines in Fig. 3(a) and (c), while the averaged values of  $d_{\text{eff}}$  for different signal polarizations along the  $x$  and  $y$  axes are shown as the thick lines. Fig. 3(b) and (d) give the corresponding averaged  $\mathcal{F}^2(\Delta k)$  covering the whole beam cross section by performing FFT, respectively. Since the high-amplitude range related to appreciable conversion efficiency spreads continuously over a wide range of  $\Delta k/2\pi$ , broadband RQPM nonlinear conversions are permitted.

A further study comes to the Monte Carlo statistical analysis of the whole polycrystalline sample, which has an average grain

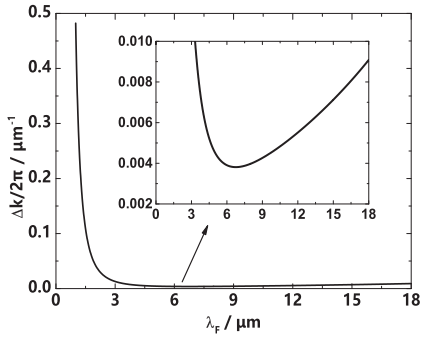


Fig. 5.  $\Delta k/2\pi$  versus fundamental wavelength  $\lambda_F$  of the SHG process in polycrystalline ZnSe. The inset is the range of  $\Delta k/2\pi$  smaller than  $0.01 \mu\text{m}^{-1}$ .

size ( $\mu$ ) of  $95 \mu\text{m}$  and standard deviation ( $\sigma$ ) of  $48 \mu\text{m}$ . All the 25 samples have the same size of  $1 \text{ mm} \times 1 \text{ mm} \times 0.5 \text{ mm}$  and each sample has  $10^4$  paths with the meshing step of  $10 \mu\text{m}$ . That is, a quarter million FFTs were performed to give the results in Fig. 4. It is believed the sample capacity guarantees the simulation reliability, from which the accurate characteristics of various RQPM interactions can be concluded. All we need to know is the value of  $\Delta k/2\pi$  for a specific nonlinear process.

### III. CHARACTERIZATION OF RQPM SHG BY THE FOURIER TRANSFORM TREATMENT

The wavelength range of the fundamental wave ( $\lambda_F$ ) in SHG was considered from  $1 \mu\text{m}$  to  $18 \mu\text{m}$  since the transparent range of polycrystalline ZnSe ( $\mu = 95 \mu\text{m}$  and  $\sigma = 48 \mu\text{m}$ ) is from  $0.55 \mu\text{m}$  to  $18 \mu\text{m}$ . Firstly, the spatial frequency mismatch  $\Delta k/2\pi$  was calculated based on the Sellmeier equation [16], where  $\Delta k = k_{\text{SHG}} - 2k_F$ . The relation of  $\Delta k/2\pi$  versus  $\lambda_F$  is shown in Fig. 5. Referring to Fig. 4, smaller  $\Delta k/2\pi$  (e.g., less than  $0.01 \mu\text{m}^{-1}$ ) yields higher efficiency, thus the RQPM SHG efficiency for wavelengths shorter than  $3.3 \mu\text{m}$  should be quite low. Moreover, that  $\Delta k/2\pi$  firstly decreases and then increases with wavelength indicates there is a peak on the SHG efficiency curve.

Combining Figs. 4 and 5, the wavelength dependent  $\mathcal{F}^2(\Delta k)$  and the intensity of the second harmonic wave can be calculated from the electric field given by (5). The results are shown in Fig. 6. The fundamental laser was assumed to be  $x$ -polarized

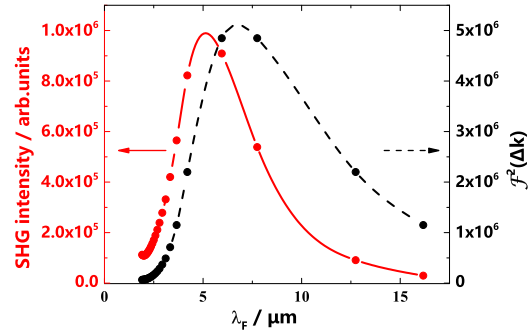


Fig. 6. The dependence of SHG intensity and  $\mathcal{F}^2(\Delta k)$  on fundamental wavelength  $\lambda_F$ .

plane-wave and the intensity was defined as unit power in a grid size ( $10 \mu\text{m} \times 10 \mu\text{m}$ ). The SHG fields of both the  $x$  and  $y$  polarizations are included by directly summing their intensities. Compared with the results calculated by the step-by-step integration method [10], the Fourier transform treatment produced the same SHG profile and demonstrated the broad bandwidth of RQPM SHG. A minor difference is that the FFT method cannot reach the short wavelength end because the values of  $\Delta k/2\pi$  are beyond the upper limit of  $0.05 \mu\text{m}^{-1}$ . Decreasing the sampling period or using spline interpolation will increase the data points and thus the wavelength range on the curves can be effectively expanded.

#### IV. ANALYSIS OF THE WAVELENGTH-TUNABLE RQPM DFG PROCESS

To fully investigate a DFG process ( $\omega_1 - \omega_2 \rightarrow \omega_3$ ), both the incident wavelengths ( $\lambda_1$  and  $\lambda_2$ ) should be tuned over the transparent range and much higher calculation amount is required even for a single-path interaction. The Fourier transform treatment provides a shortcut and makes the accurate characterization of RQPM DFG become reality. FFT directly gives the values of spatial frequency mismatch  $\Delta k/2\pi$  for all the DFG processes once the detailed morphology of the polycrystalline sample is confirmed. The rest is to check the relation of  $\Delta k/2\pi$  to wavelengths ( $\lambda_1$  and  $\lambda_2$ ) and calculate the field intensity of the generated wavelength ( $\lambda_3$ ) from (5). The parameters of the polycrystalline ZnSe sample and incident beam intensity are the same as those in studying the SHG process.

The colored mapping of  $\Delta k/2\pi$  for DFG is shown in Fig. 7(a), where all the possible DFG interactions are considered by fully scanning  $\lambda_1$  and  $\lambda_2$ . The areas beyond the transparent range, whether for  $\lambda_1$ ,  $\lambda_2$  or  $\lambda_3$ , were all set zero here. Similar to Fig. 4, the smaller value of  $\Delta k/2\pi$ , the higher  $\mathcal{F}^2(\Delta k)$  given in Fig. 7(b), and thus the higher photon conversion efficiency. Obviously, the maximum photon conversion efficiency occurs when the pump wavelength  $\lambda_1$  is in the  $2\text{--}4 \mu\text{m}$  range and the generated wavelength  $\lambda_3$  is in the  $3\text{--}9 \mu\text{m}$  range. The wavelength-dependent coherence length of DFG in ZnSe given in Fig. 7(c) also supports such a result, as the grain size with lognormal distribution mostly spreads from  $40 \mu\text{m}$  to  $130 \mu\text{m}$  to match the coherence length. The power conversion efficiency (or the generated signal intensity shown in Fig. 7(d)), has a

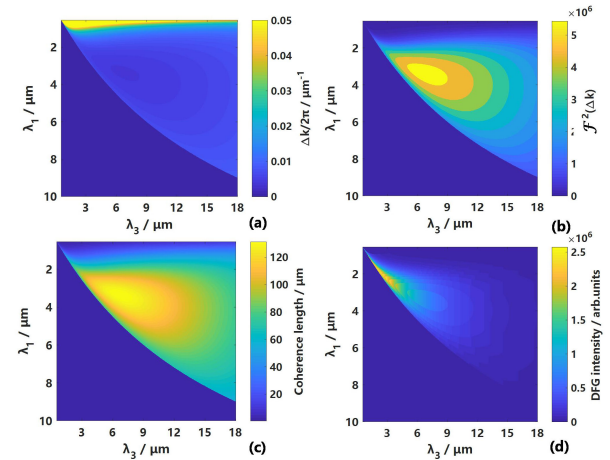


Fig. 7. Colormaps of the DFG process in polycrystalline ZnSe with Fourier transform treatment. (a) Spatial frequency mismatch,  $\Delta k/2\pi$ . (b) Square of FFT amplitude,  $\mathcal{F}^2(\Delta k)$ . (c) Coherence length. (d) Generated signal intensity.

distribution that is quite different to that in Fig. 7(b), because the frequency weights a lot according to (4) and (5). The highest efficiency is obtained when the pump wavelength  $\lambda_1$  is from  $1.2 \mu\text{m}$  to  $2.7 \mu\text{m}$ . and the corresponding generated wavelength  $\lambda_3$  is from  $1.3 \mu\text{m}$  to  $3.5 \mu\text{m}$ . The results should help to determine the optimal condition of a broadband MIR source via RQPM DFG.

To evaluate the calculation amount of the Fourier transform treatment, a single-beam-path interaction along a  $500\text{-}\mu\text{m}$ -thick polycrystalline model with the meshing step of  $10 \mu\text{m}$  is considered. Based on the basic butterfly computation algorithm of FFT [15], [17], there are complex multiplications of

$$n = \frac{N}{2} \log_2 N, \quad (6)$$

where  $N = 51$  is the data points for  $d_{\text{eff}}$  along the beam path. That is, 145 complex multiplications are needed to acquire the preliminary result. All the additional work is the conversion from wavelength to spatial frequency mismatch  $\Delta k/2\pi$ , which introduces little computational load and can be ignored basically. However, the same results require the direct step-by-step integration method to perform wavelength scanning for both  $\lambda_1$  and  $\lambda_2$  over the whole transparent range. That is, the DFG process needs  $25 \times 25 \times 50 = 31250$  integrations, where 25 is the number of wavelength points during scanning, which is consistent with the FFT process. Undoubtedly, the Fourier transform treatment greatly simplifies the calculation.

Moreover, the Fourier transform treatment for RQPM includes various three-wave interactions (SHG, DFG, etc.) simultaneously, as the critical variable is  $\Delta k$  rather than the wavelength. Accurate wavelength dependence needs dense sampling in the entire transparent range. If the wavelength points are increased, the calculation with the direct integration method would be increased quadratically, while it is merely a logarithmic increase for the FFT process. Thus, the advantage of the Fourier transform treatment becomes more distinct in high-resolution wavelength dependent simulations.

## V. CONCLUSION

The Fourier transform approach is employed in the analysis of RQPM processes by treating the polycrystalline material as random signals of effective nonlinear coefficient ( $d_{\text{eff}}$ ) along the beam path. The FFT operation provides the relative amplitude of the generated field that relates to the spatial frequency mismatch ( $\Delta k/2\pi$ ). Once the FFT is performed, it is treated as a lookup table that applies to all the possible RQPM nonlinear interactions along the same beam path. In addition, the calculation amount can be greatly decreased by orders compared with the conventional step-by-step integration method. The study on RQPM SHG proves the accuracy and feasibility of the Fourier transform treatment with a specific polycrystalline ZnSe model generated by Neper. And, attributed to the efficient method, the quantitative simulation of RQPM DFG interactions with two variable wavelengths was realized for the first time to intuitively predict the wavelength dependent output characteristics.

## REFERENCES

- [1] M. Baudrier-Raybaut, R. Haïdar, P. Kupecek, P. Lemasson, and E. Rosenthaler, "Random quasi-phase-matching in bulk polycrystalline isotropic nonlinear materials," *Nature*, vol. 432, no. 7015, pp. 374–376, Nov. 2004, doi: [10.1038/nature03027](https://doi.org/10.1038/nature03027).
- [2] K. Werner *et al.*, "Ultrafast mid-infrared high harmonic and supercontinuum generation with  $n_2$  characterization in zinc selenide," *Opt. Exp.*, vol. 27, no. 3, pp. 2867–2885, Feb. 2019, doi: [10.1364/OE.27.002867](https://doi.org/10.1364/OE.27.002867).
- [3] Q. Ru *et al.*, "Optical parametric oscillation in a random polycrystalline medium," *Optica*, vol. 4, no. 7, pp. 617–618, Jul. 2017, doi: [10.1364/OPTICA.4.000813](https://doi.org/10.1364/OPTICA.4.000813).
- [4] Q. Ru *et al.*, "Optical parametric oscillation in a random poly-crystalline medium: Znse ceramic," in *Proc. SPIE*, San Francisco, CA, USA, Feb. 2018, Art. no. 1051615.
- [5] J. Zhang, K. Fritsch, Q. Wang, F. Krausz, K. F. Mak, and O. Pronin, "Intra-pulse difference-frequency generation of mid-infrared (2.7–20  $\mu\text{m}$ ) by random quasi-phase-matching," *Opt. Lett.*, vol. 44, no. 12, pp. 2986–2989, Jun. 2019, doi: [10.1364/OL.44.002986](https://doi.org/10.1364/OL.44.002986).
- [6] S. Vasilyev *et al.*, "Octave-spanning Cr:ZnS femtosecond laser with intrinsic nonlinear interferometry," *Optica*, vol. 6, no. 2, pp. 126–127, Jan. 2019, doi: [10.1364/OPTICA.6.000126](https://doi.org/10.1364/OPTICA.6.000126).
- [7] J. Trull *et al.*, "Second-harmonic parametric scattering in ferroelectric crystals with disordered nonlinear domain structures," *Opt. Exp.*, vol. 15, no. 24, pp. 15868–15877, Nov. 2007, doi: [10.1364/OE.15.015868](https://doi.org/10.1364/OE.15.015868).
- [8] T. Kawamori T, Q. Ru, and K. L. Vodopyanov, "Comprehensive model for randomly phase-matched frequency conversion in zinc-blende polycrystals and experimental results for ZnSe," *Phys. Rev. Appl.*, vol. 11, no. 5, May 2019, Art. no. 054015, doi: [10.1103/PhysRevApplied.11.054015](https://doi.org/10.1103/PhysRevApplied.11.054015).
- [9] J. Gu, M. Hastings, and M. Kolesik, "Simulation of harmonic and supercontinuum generation in polycrystalline media," *J. Opt. Soc. Amer. B*, vol. 37, no. 5, pp. 1510–1517, May 2020, doi: [10.1364/JOSAB.388914](https://doi.org/10.1364/JOSAB.388914).
- [10] K. Liu, K. Zhong, and Z. Lu, "Effects of grain morphology on nonlinear conversion efficiency of random quasi-phase matching in polycrystalline materials," *IEEE Photon. J.*, vol. 12, no. 6, Jan. 2020, Art. no. 2200910, doi: [10.1109/JPHOT.2020.3034358](https://doi.org/10.1109/JPHOT.2020.3034358).
- [11] R. Quey and R. L. Renversade, "Optimal polyhedral description of 3D polycrystals: Method and application to statistical and synchrotron X-ray diffraction data," *Comput. Methods Appl. Mech. Eng.*, vol. 330, pp. 308–333, Mar. 2018, doi: [10.1016/j.cma.2017.10.029](https://doi.org/10.1016/j.cma.2017.10.029).
- [12] A. Tehranchi and R. Kashyap, "Engineered gratings for flat broadening of second-harmonic phase-matching bandwidth in MgO-doped lithium niobate waveguides," *Opt. Exp.*, vol. 16, no. 23, pp. 18970–18975, Nov. 2008, doi: [10.1364/OE.16.018970](https://doi.org/10.1364/OE.16.018970).
- [13] P. E. Powers and J. W. Haus, *Fundamentals of Nonlinear Optics*, 2nd ed. Boca Raton, FL, USA: CRC Press, Taylor & Francis Group, 2017.
- [14] M. M. Fejer, G. A. Magel, and D. H. Jundt, "Quasi-phase-matched second harmonic generation: Tuning and tolerances," *IEEE J. Quantum Electron.*, vol. 28, no. 11, pp. 2631–2654, Nov. 1992, doi: [10.1109/3.161322](https://doi.org/10.1109/3.161322).
- [15] A. V. Oppenheim, "Discrete-time signal processing," in *Pearson Education*, 1st ed., Hoboken, NJ, USA: Prentice Hall, 1999.
- [16] H. H. Li, "Refractive index of ZnS, ZnSe, and ZnTe and its wavelength and temperature," *J. Phys. Chem. Ref. Data*, vol. 13, no. 1, pp. 103–150, Jan. 1984, doi: [10.1063/1.555705](https://doi.org/10.1063/1.555705).
- [17] J. W. Cooley and J. W. Tukey, "An algorithm for the machine calculation of complex Fourier series," *Math. Comput.*, vol. 19, no. 90, pp. 297–301, Apr. 1965, doi: [10.2307/2003354](https://doi.org/10.2307/2003354).